

Stabilization of YMnO₃ in a Perovskite Structure as a Thin Film

Paul A. Salvador, Trong-Duc Doan,
Bernard Mercey,* and Bernard Raveau

Laboratoire CRISMAT, CNRS UMR 6508, ISMRA,
Université de Caen, 6, Boulevard du Maréchal Juin,
14050 Caen Cedex, France

Received April 14, 1998

Revised Manuscript Received June 16, 1998

The ability to design technologically useful and scientifically interesting materials based on chemical principles is an important goal in the field of materials chemistry, particularly for solid-state materials. An important factor in the stabilization of particular structures and/or phases is the synthetic pathway. Pulsed laser deposition (PLD) of thin films has been used as an effective alternative to high-pressure or soft-chemical techniques for synthesizing metastable phases.^{1–3} For example, metastable layered copper oxides, such as the AECuO₂ (AE = Ca, Sr, Ba) phases,^{4–9} other copper-based perovskites,^{10–12} and complex, superconducting oxycarbonates,^{13,14} have been synthesized via PLD. Moreover, artificial structures and superlattices of these phases have been attained owing to the unique synthetic aspects of thin-film deposition.^{1,3,14} Thin-film-deposition techniques are ideally suited to synthesizing materials whose metastable structure is similar to that of the substrate and/or has novel two-dimensional cationic order that is often impossible to achieve with either classical powder or high-pressure synthetic techniques.^{3,15}

In this paper we report the synthesis of a metastable form of the manganese oxide YMnO₃ by PLD. Although metastable forms of many copper oxides have already been synthesized by various thin-film techniques, it remains to be shown how versatile these approaches are

with respect to other metastable transition metal oxides. PLD has been widely used to deposit films of various manganese perovskites of the nominal formula Ln_{1-x}AE_xMnO₃ (Ln = lanthanide, Y; AE = alkaline earth),^{16–22} because of their interesting structural, electronic, and magnetic properties, in particular, colossal magnetoresistance. However, when the average size of the Ln and AE cations is extremely small, such as for YMnO₃, the perovskite structure is destabilized under synthetic conditions of atmospheric pressure and high temperatures.²³ The hexagonal YMnO₃ structure, shown in Figure 1 (space group *P6₃cm*, *a* = 6.125, *c* = 11.41),²³ is obtained instead. This structure is best described as layers of manganese-centered trigonal bipyramids (5-coordinate manganese) which have no framework Mn–O bonds along their axial direction (*c*-axis; see Figure 1a) and corner share the equatorial oxygen between three polyhedra (in the basal plane; see Figure 1b).

High-pressure synthesis or low-temperature soft-chemistry synthesis can be used to stabilize the close-packed perovskite lattice for YMnO₃, whose orthorhombic structure (space group *Pnma*, *a* = $\sqrt{2}a_p$ = 5.26, *b* = $2a_p$ = 7.35, *c* = $\sqrt{2}a_p$ = 5.84; note that *a_p* signifies the approximate cell parameter for a cubic perovskite, ≈ 3.9 Å)^{24–26} is shown in Figure 2. The highly distorted nature of the corner-sharing octahedral network is emphasized through the two different orientations in Figure 2: part a emphasizes the [010] direction and b emphasizes the [101] direction. With the current interest in manganese oxides, for their colossal magnetoresistance, the stabilization of the metastable variants is important for extending our knowledge of structure–property relationships. In addition, the ability to create artificially layered structures with atomic-level control using PLD techniques, as demonstrated with copper oxides, may also allow for uniquely ordered manganese oxides to be investigated with respect to their structure–property relationships. As a first step toward achieving these goals, we investigated the synthesis and structure of YMnO₃ films synthesized using the PLD technique. While the hexagonal form of YMnO₃ has already been realized as a thin film,^{27,28} the high-pressure perovskite form has not been stabilized to date as a thin film.

* Author to whom correspondence should be addressed. E-mail: mercey@crismat.ismra.fr. Tel: (33) 2-31-45-26-08. Fax: (33) 2-31-95-16-00.

- (1) Kawai, T.; Egami, Y.; Tabata, H.; Kawai, S. *Nature* **1991**, *349*, 200.
- (2) Lowndes, D. H.; Goehagan, D. B.; Puretzy, A. A.; Norton, D. P.; Rouleau, C. M. *Science* **1996**, *273*, 898–903.
- (3) Gupta, A. *Curr. Opin. Solid State Mater. Sci.* **1997**, *2*, 23–31.
- (4) Kanai, M.; Kawai, T.; Kawai, S. *Appl. Phys. Lett.* **1991**, *58*, 771–773.
- (5) Niu, C.; Lieber, C. M. *Appl. Phys. Lett.* **1992**, *61*, 1712–1714.
- (6) Niu, C.; Lieber, C. M. *J. Am. Chem. Soc.* **1993**, *115*, 137–144.
- (7) Norton, D. P.; Chakoumakos, B. C.; Budai, J. D.; Lowndes, D. H. *Appl. Phys. Lett.* **1993**, *62*, 1679–1681.
- (8) Gupta, A.; Hussey, B. W.; Shaw, T. M.; Guloy, A. M.; Chern, M. Y.; Saraf, R. F.; Scott, B. A. *J. Solid State Chem.* **1994**, *112*, 113–119.
- (9) Gupta, A. *Physica C* **1994**, *231*, 389–394.
- (10) Gupta, A.; Mercey, B.; Hervieu, M.; Raveau, B. *Chem. Mater.* **1994**, *6*, 1011–1016.
- (11) Gupta, A.; Hussey, B. W.; Guloy, A. M.; Shaw, T. M.; Saraf, R. F.; Bringley, J. F.; Scott, B. A. *J. Solid State Chem.* **1994**, *108*, 202–206.
- (12) Desfeux, R.; Hamet, J. F.; Mercey, B.; Simon, C.; Hervieu, M.; Raveau, B. *Physica C* **1994**, *221*, 205–214.
- (13) Allen, J. L.; Mercey, B.; Prellier, W.; Hamet, J. F.; Hervieu, M.; Raveau, B. *Physica C* **1995**, *241*, 158–166.
- (14) Prellier, W.; Mercey, B.; Lecoeur, P.; Hamet, J. F.; Raveau, B. *Appl. Phys. Lett.* **1997**, *71*, 782–784.
- (15) *Pulsed Laser Deposition of Thin Films*; Crisey, D. B.; Hubler, G. K., Ed.; John Wiley & Sons: New York, 1994; p 613.

(16) von Helmolt, R.; Wecker, J.; Holzapfel, R.; Schultz, L.; Samwer, K. *Phys. Rev. Lett.* **1993**, *71*, 2331–2333.

(17) Ju, H. L.; Kwon, C.; Li, Q.; Greene, R. L.; Venkatesan, T. *Appl. Phys. Lett.* **1994**, *65*, 2108–2110.

(18) McCormack, M.; Jin, S.; Tiefel, T. H.; Fleming, R. M.; Philips, J. M.; Ramesh, R. *Appl. Phys. Lett.* **1994**, *64*, 3045–3047.

(19) Xiong, G. C.; Li, Q.; Ju, H. L.; Greene, R. L.; Venkatesan, T. *Appl. Phys. Lett.* **1995**, *66*, 1689–1691.

(20) Xiong, G. C.; Li, Q.; Ju, H. L.; Greene, R. L.; Venkatesan, T. *Appl. Phys. Lett.* **1995**, *66*, 1427–1429.

(21) Sun, J. Z.; Krusin-Elbaum, L.; Parkin, S. S. P.; Xiao, G. *Appl. Phys. Lett.* **1995**, *67*, 2726–2728.

(22) McGuire, T. R.; Gupta, A.; Duncombe, P. R.; Rupp, M.; Sun, J. Z.; Laibowitz, R. B.; Gallagher, W. J. *J. Appl. Phys.* **1996**, *79*, 4549–4551.

(23) Yakel, H. L.; Koehler, W. C.; Bertaut, E. F.; Forrat, E. F. *Acta Crystallogr.* **1963**, *16*, 957–962.

(24) Waintal, A.; Chenavas, J. C. R. *Acad. Sci. Paris, Ser. B* **1967**, *264*, 168–170.

(25) Waintal, A.; Chenavas, J. *Mater. Res. Bull.* **1967**, *2*, 819–822.

(26) Iliev, M. N.; Abrashev, M. V.; Lee, H.-G.; Popov, V. N.; Sun, Y. Y.; Thomsen, C.; Meng, R. L.; Chu, C. W. *Phys. Rev. B* **1998**, *57*, 2872–2877.

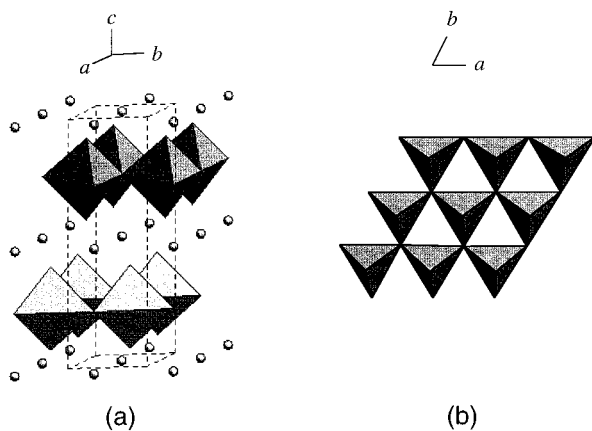


Figure 1. Polyhedral representation of the structure of the hexagonal form of YMnO_3 . The spheres represent the Y^{3+} cations while the Mn^{3+} cations reside near the center of the 5-coordinate polyhedra and the O^{2-} anions at the apexes of the polyhedra. Axial directions are marked above the figures. In panel a, emphasis is on the interlayer orientations and lack of Mn–O connectivity in the c -direction, while in panel b, the emphasis is placed on the in-plane (a,b -plane) Mn–O connectivity between the trigonal bipyramids.

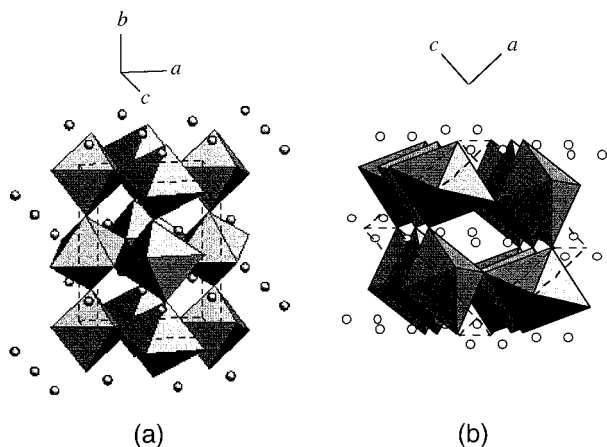


Figure 2. Polyhedral representation of the structure of the orthorhombic form of YMnO_3 . The spheres represent the Y^{3+} cations while the Mn^{3+} cations reside near the center of the 6-coordinate polyhedra and the O^{2-} anions at the apexes of the polyhedra. Axial directions are marked above the figures. In panel a, the $[010]$ direction is emphasized, while in panel b, the $[101]$ direction is emphasized. Note that the cooperative rotations of the corner-sharing octahedra lead to distinct differences in these directions, both of which are derived from the axial directions of the nondistorted cubic perovskite subcell.

A dense target of hexagonal YMnO_3 was synthesized via standard ceramic synthesis methods. Y_2O_3 and MnO_2 were mixed in the appropriate ratios and intimately ground using a semiplanetary ball mill. The powder was annealed twice for 12 h at 900 °C and once for 12 h at 1200 °C, with intermediate grindings. Heating and cooling rates were 100 °C/h. The pellet was isostatically pressed when cold and sintered at 1500 °C for 12 h, where heating and cooling rates of 80 °C/h were used. The hexagonal phase was identified as the main target phase by Guinier powder diffraction.

The PLD apparatus used for deposition is described elsewhere.^{13,14} Some of the important deposition parameters are $\lambda = 248$ nm, pulse rate = 3 Hz, laser power density = 2 J/cm², target to substrate distance = 47 mm. Films were deposited on single-crystal substrates of (100) SrTiO_3 , (100) LaAlO_3 , and (110) NdGaO_3 which, during deposition, were held at a constant temperature ranging from 600 to 725 °C in a dynamic vacuum having an O_2 pressure ranging from 0.27 to 0.53 mbar. The optical quality substrates were ultrasonically cleaned in acetone and then in alcohol and were attached to the heater using silver paste. A type K thermocouple was mechanically attached to the heater block close to the substrates and the temperature measured at this location is referred to as the deposition temperature. The background pressure of the chamber was 10^{-5} mbar. After deposition was completed, the oxygen pressure was increased to a static value of 300 mbar, and the films were cooled to room temperature at 20 °C/min.

The resulting films were transparent with a slight brownish tint and mirrorlike surfaces. X-ray diffraction (XRD) patterns were collected using a Seiffert XRD 300 diffractometer with $\text{Cu K}\alpha_1$ radiation. Parts a and b of Figure 3 show the XRD patterns of YMnO_3 deposited on SrTiO_3 and NdGaO_3 , respectively, at a temperature of 725 °C and an oxygen pressure of 0.53 mbar. Films deposited on SrTiO_3 substrates exhibit peaks consistent with the $(0k0)$ planes of the orthorhombic perovskite ($k = 2, 4; 2\theta = 24.15^\circ, 49.46^\circ$), and the b -axis length is calculated to be 7.364(6) Å (the number in parentheses indicates the error on last digit), in agreement with literature values.^{24–26} In contrast, films deposited on NdGaO_3 substrates exhibit peaks consistent with the $(h0l)$ planes ($h = l = 1, 2; 2\theta = 22.82^\circ, 46.62^\circ$) of the orthorhombic structure. The $[101]$ distance is calculated to be $\approx 3.894(3)$ Å, in agreement with literature values (i.e., 3.902 Å^{24–26,29}). Films deposited on LaAlO_3 substrates (not shown) were similar to those deposited on NdGaO_3 substrates, although both orientations ($[101]$ and $[010]$) were observed in some cases. At lower temperatures (620 °C) films were poorly crystalline on all substrates, but at temperatures above 675 °C (until our experimental limit near 725 °C), XRD patterns similar to those in Figure 3 were observed. In all cases, no diffraction peaks from the hexagonal form, the constituent oxides, or the pyrochlore phase³⁰ were observed.

TEM experiments were carried out to confirm the epitaxial nature of these films and to investigate their structural characteristics in the plane of the substrate. Transmission electron microscopy (TEM) was carried out using a JEOL 200 CX microscope, equipped with an energy-dispersive spectroscopy (EDS) analyzer (KEVEX) to determine the film stoichiometry. Films were also observed using a Philips XL30 FEG scanning electron microscopy (SEM) coupled with EDS (Oxford) to observe their microstructural quality and compositional homogeneity. EDS coupled to SEM and TEM indicated that the film stoichiometry was homogeneous and was identical to that of the nominal target stoichi-

(27) Fujimura, N.; Azuma, S.-I.; Aoki, N.; Yoshimura, T.; Ito, T. *J. Appl. Phys.* **1996**, *80*, 7084–7088.

(28) Fujimura, N.; Ishida, T.; Yoshimura, T.; Ito, T. *Appl. Phys. Lett.* **1996**, *69*, 1011–1013.

(29) Brinks, H. W.; Fjellvåg, H.; Kjekshus, A. *J. Solid State Chem.* **1997**, *129*, 334–340.

(30) Subramanian, M. A.; Torardi, C. C.; Johnson, D. C.; Pannetier, J.; Sleight, A. W. *J. Solid State Chem.* **1988**, *72*, 24–30.

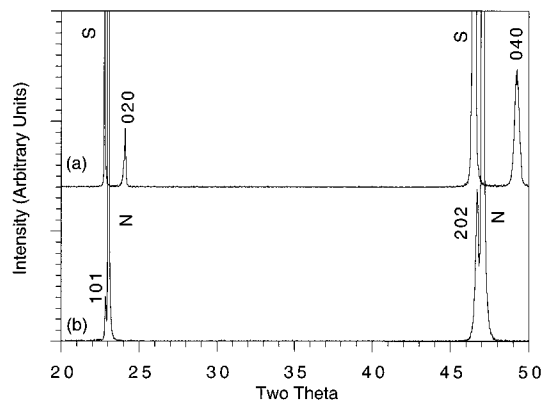


Figure 3. XRD patterns of epitaxial YMnO_3 films on (a) SrTiO_3 and (b) NdGaO_3 . S denotes the reflections from SrTiO_3 and N the reflections from NdGaO_3 . The peaks from the orthorhombic perovskite form of YMnO_3 are denoted with respect to the appropriate reflections from the bulk form.

ometry, i.e., $\text{Y:Mn} \approx 1:1$, within the 1% detection limit on our equipment.

Figure 4a is the selected area diffraction pattern (SAED) of the $[010]$ zone, i.e., in the plane of the substrate, for the film whose XRD pattern was given in Figure 3a. Surprisingly, the 4-fold symmetry observed in this SAED pattern does not correspond to that expected for the orthorhombic structure of the known perovskite form of YMnO_3 . Yet, the 4-fold symmetry of this zone axis is consistent with the perovskite structure itself and can be indexed as shown in the figure with $a \approx c \approx \sqrt{2}a_p = 5.24 \text{ \AA}$ ($a_p \approx 3.89(1) \text{ \AA}$). The $h00$ and $00l$ spots having $h, l = \text{odd}$ are not extinct, as expected for the $Pnma$ space group, but are instead faintly present and are likely the result of double-diffraction phenomena. Diffuse streaking of the diffraction spots is also observed and indicates that the long-range symmetry is somewhat disordered. This also implies that the observed 4-fold symmetry may not be a true indication of the film symmetry but that, for the case of these 680 \AA films, the films are highly strained owing to the substrate symmetry (cubic, $a_p = 3.905 \text{ \AA}$). There was no indication of the existence of domains containing the long axis, corresponding to $b = 2a_p = 7.364(6) \text{ \AA}$, in the plane of the substrate, which is consistent with the XRD patterns. These results confirm the overall perovskite-like structure of this metastable YMnO_3 phase. Yet, the lack of an obvious orthorhombic symmetry and the occurrence of the odd h, l spots may indicate that the true symmetry of these epitaxial films is more complicated than that previously reported for the perovskite-like variant of this phase.^{24–26,29}

A SAED pattern, corresponding to the $[101]$ zone from the film whose XRD pattern is given in Figure 3b, is shown in Figure 4b. In this case, a distance corresponding to the longer b -parameter is observed in the plane of the substrate, i.e., $b = 2a_p = 7.33(1) \text{ \AA}$, and is consistent with the XRD results. The occurrence of the $0k0$ spots where $k = \text{odd}$ (which should be extinct for the $Pnma$ space group) is most likely a result of double diffraction phenomena. The $[\bar{1}01]$ distance is calculated to be $\approx 3.90(1) \text{ \AA}$ from this image, and is in agreement with the $[101]$ distance calculated from the XRD pattern ($3.894(3) \text{ \AA}$). No regions of the sample were found where the SAED patterns evinced the existence of 90° oriented

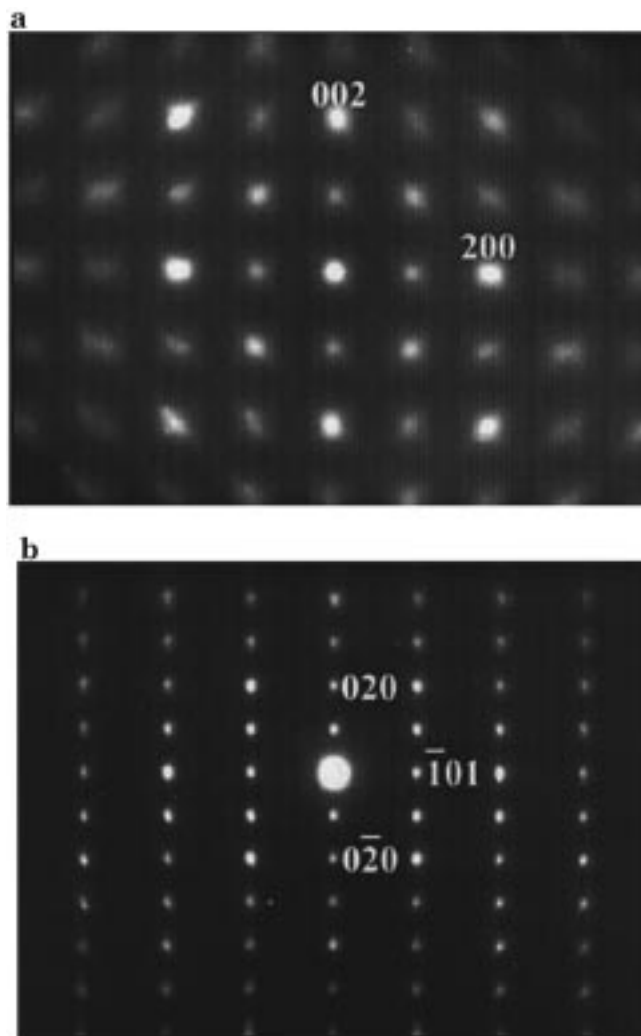


Figure 4. Selected area electron diffraction images in the substrate plane of YMnO_3 films on (a) SrTiO_3 and (b) NdGaO_3 . The reflections are marked with respect to the appropriate principle reflections allowed for the $Pnma$ space group observed for the bulk material. The existence of the $h00$, $0k0$, or $00l$ peaks having an odd index can be attributed to double diffraction phenomena (see the text).

domains. In addition, TEM images indicated that the long axis was well-oriented with respect to a single direction of the substrate, i.e., no 90° domains were observed. The corresponding microstructure was highly granular with very small grain sizes, $\approx 250\text{--}300 \text{ \AA}$ (but identical orientations for all grains). The large difference of the $b/2$ ($\approx 3.67(1) \text{ \AA}$) and $[\bar{1}01]$ ($\approx 3.90(1) \text{ \AA}$) distances, of the film, leads to a single in-plane orientation of the film with respect to the substrate. The film axes are most likely aligned with the same axes of the substrate (i.e., $[010]^{\text{film}} \parallel [010]^{\text{sub}}$ and $[\bar{1}01]^{\text{film}} \parallel [\bar{1}01]^{\text{sub}}$), whose respective distances are $b/2^{\text{NGO}} \approx 3.85 \text{ \AA}$ and $[\bar{1}01]^{\text{NGO}} \approx 3.87 \text{ \AA}$.³¹ These results confirm that the epitaxial films deposited on NdGaO_3 do indeed adopt a perovskite structure which has lattice parameters in good agreement with the literature values of the orthorhombic phase. However, from the data presented here it is impossible to confirm whether the true symmetry is tetragonal or orthorhombic.

(31) Marti, W.; Fischer, P.; Altofer, F.; Schell, H. J.; Tadin, M. J. *Phys.: Cond. Matter* **1994**, *6*, 127–135.

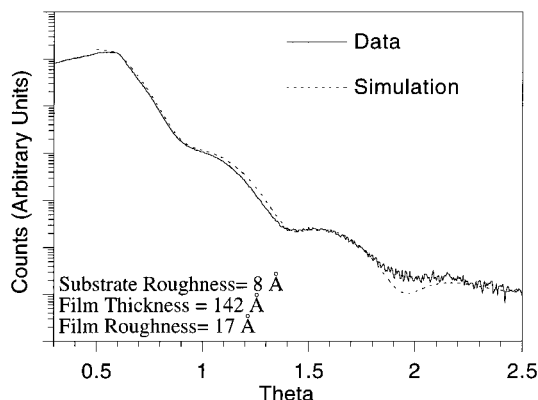


Figure 5. Grazing incidence X-ray diffraction data and simulation for a thin film of YMnO_3 deposited on SrTiO_3 . Refined parameters are provided in the plot.

Grazing incidence X-ray diffraction was carried out using a Philips X'pert MRD diffractometer with Cu radiation. Figure 5 shows the thus collected data and calculated fits, simulated with the GIXA software (Philips), for an extremely thin YMnO_3 film. Theoretical values of the real and imaginary parts of the refractive index³² for the perovskite structure of YMnO_3 (using the experimentally observed unit cell volume) fit the data well. Since they did not vary during the refinement, they were held constant at the initial values. Surface roughness of the substrate and both the thickness and the surface roughness of the film were refined along with the initial intensity, angular offset, and background intensity. Substrate roughness refined to $\approx 8 \text{ \AA}$ (≈ 2 cells) and is consistent with the substrate quality. The thickness is determined to be 142 \AA , which results in a deposition rate of $0.14(1) \text{ \AA/laser pulse}$ (25 \AA/min). The surface roughness was calculated to be $\approx 17 \text{ \AA}$. Reflectometry on a thicker film, whose XRD pattern is given in Figure 3a, yielded the same deposition rate, a

(32) James, R. W. *The Optical Principles of the Diffraction of X-rays*; Cornell University Press: Ithica, 1955.

thickness of 680 \AA , and only slightly larger surface roughness (roughness values were $\approx 5\%$ of the thickness).

These results demonstrate that epitaxial films having a perovskite-like structure could be obtained for YMnO_3 by PLD. Considering the previous reports on the thin-film synthesis of the hexagonal form of YMnO_3 ,^{27,28} we find that the choice of the substrate controls not only the structure but also the epitaxial nature of the films. Using perovskite substrates and a PLD technique, we have been able to obtain smooth, epitaxial films whose orientation varies with respect to the substrate. Films on SrTiO_3 have an in-plane symmetry which is similar to that of the substrate (i.e., 4-fold) and this implies that the film is highly strained and that the cooperative rotations of the octahedra, which lead to orthorhombic symmetry in bulk YMnO_3 perovskites, are not completely relaxed. However, the films on NdGaO_3 substrates exhibit lattice parameters which are similar to those of the orthorhombic form of YMnO_3 , and preferential lattice matching of the axes with the substrate leads to granular type growth with well-crystallized, albeit small, in-plane oriented grains. Stabilization of this metastable phase demonstrates that the $\text{Y}_{1-x}\text{AE}_x\text{MnO}_3$ phases can be investigated as epitaxial perovskite films even in regions where standard synthetic methods lead to nonperovskite structures. Moreover, the low deposition rate and smooth surfaces which are obtained imply that novel cationic order in the manganese oxides may be realizable with this system as a component using the PLD technique. Finally, these results imply that metastable perovskites may be attainable in more complex systems of interest, in which the thermodynamically stable phase under standard synthesis conditions is the hexagonal YMnO_3 type.

Acknowledgment. P.A.S. gratefully acknowledges the financial support of the Chateaubriand Fellowship and CNRS.

CM9802797